ELSEVIER

Journal of Alloys and Compounds 446–447 (2007) 625–629

Journal of ALLOYS AND COMPOUNDS

www.elsevier.com/locate/jallcom

Effects of Cr addition on the microstructures and electrochemical performances of La–Mg–Ni system ($PuNi_3$-type) hydrogen storage alloy

Xin-lin Wang [a], Yang-huan Zhang [a,b,*], Dong-liang Zhao [a],
Xiao-ping Dong [a,c], Shi-hai Guo [a], Guo-qing Wang [a]

[a] *Department of Functional Material Research, Central Iron and Steel Research Institute, Beijing, PR China*
[b] *School of Material, Inner Mongolia University of Science and Technology, Baotou, PR China*
[c] *School of Material Science and Engineering, University of Science and Technology Beijing, 100083 Beijing, PR China*

Received 19 October 2006; received in revised form 12 January 2007; accepted 12 January 2007
Available online 18 January 2007

Abstract

In order to improve the electrochemical cycle stability of La–Mg–Ni system ($PuNi_3$-type) hydrogen storage alloy, a trace of Cr was added in the alloy and $La_2Mg(Ni_{0.85}Co_{0.15})_9Cr_x$ ($x = 0$, 0.1, 0.2, 0.3, 0.4) hydrogen storage alloys were prepared by casting and rapid quenching. The effects of Cr addition on the microstructures and electrochemical performances of the as-cast and quenched alloys were investigated in detail. The obtained results show that Cr addition engenders an inappreciable influence on the phase composition of the as-cast and quenched alloys, but it changes the phase abundance of the alloys significant. The Cr addition markedly enhances the cycle stability of the as-cast and quenched alloys, but it decreases the discharge capacity. When Cr content increased from 0 to 0.4, the discharge capacity of the as-cast alloy decreased from 396.3 to 355.6 mAh/g, and the cycle life prolonged from 72 to 97 cycles. For the as-quenched (30 m/s) alloys, the discharge capacity reduced from 364.2 to 334.2 mAh/g, and the cycle life extended from 100 to 131 cycles.

Keywords: La–Mg–Ni-system hydrogen storage alloy; Cr addition; Electrochemical performances; Microstructures

1. Introduction

Intermetallic compounds for reversible hydrogen absorption/desorption have been the subject of extensive research for about 30 years. Consequently, a series of metal hydride electrode materials have been developed. Of these alloys, the AB_5-type hydrogen storage alloy has realized large-scale industrialization in many countries, such as Japan and China [1,2]. However, the rechargeable Ni-MH batteries are facing serious challenge from Li-ion cells since the Li-ion cells show higher energy density than the Ni-MH cells per unit weight or volume. Therefore, the development of the new type of electrode alloys with higher capacity and longer cycling life is remarkably important to enhance the competition ability of the Ni-MH batteries in the rechargeable battery field. Recently, several new and good hydrogen storage alloys were reported. The most promising candidates are the La–Mg–Ni system alloys owing to their higher discharge capacities (360–410 mAh/g) and low production costs. However, the rather poor cycling stability of the La–Mg–Ni system alloys has to be further improved for commercial application. For this purpose, the worldwide researchers have carried out a lot of investigations and obtained important results. Kohno et al. [3] found that the $La_5Mg_2Ni_{23}$-type electrode alloy $La_{0.7}Mg_{0.3}Ni_{2.8}Co_{0.5}$ has a capacity of 410 mAh/g and good cycle stability during 30 charge–discharge cycles. Liao et al. [4] investigated the effect of Co substitution for Ni on the structural and electrochemical properties of $La_2Mg(Ni_{1-x}Co_x)_9$ ($x = 0.1$–0.5) hydrogen storage electrode alloys and confirmed that substituting Ni with Co could obviously improve the cycle stability of the La–Mg–Ni system

---

[*] Corresponding author at: Department of Functional Material Research, Central Iron and Steel Research Institute, 76 Xueyuan Nan Road, Haidian District, 100081 Beijing, PR China. Tel.: +86 10 62187570; fax: +86 10 62182296.

E-mail addresses: wangxinlin@vip.163.com (X.-l. Wang), zyh59@yahoo.com.cn, zhangyh59@163.com (Y.-h. Zhang).

0925-8388/$ – see front matter © 2007 Elsevier B.V. All rights reserved.
doi:10.1016/j.jallcom.2007.01.062

alloys. Kadir et al. [5] investigated the structure of the R_2MgNi_9 (R = La, Ce, Pr, Nd, Sm and Gd) alloys and the obtained result shows that the alloys have the $PuNi_3$-type structure. Pan et al. [6] researched the structures and electrochemical characteristics of the $La_{0.7}Mg_{0.3}Ni_{3.4}–xMn_{0.1}Co_x$ ($x = 0–1.15$) alloys. The results indicated that the alloy ($x = 0.75$) has a maximum discharge capacity of 403.1 mAh/g, and after 30 charge–discharge cycles, the discharge capacity retention of the alloy electrodes increases obviously from 55.1 ($x = 0$) to 75.3% ($x = 1.15$) with increasing Co substitution. It is well known that the element addition and substitution is one of the effective methods for improving the overall properties of the hydrogen storage alloys [7,8] and our previous work [9,10] showed that the manufacturing technology is quite important for improving the electrochemical performances of the electrode alloys. Especially, rapid quenching leads to the marked refinement of the electrode alloy's grains and the formation of an amorphous phase, which significantly enhances the cycle stability of the alloys. Thus, it is expected that an appropriate amount of Cr addition in the La–Mg–Ni system alloy and a selected rapid quenching technique could produce an alloy with good cycling stability. Therefore, this paper systematically investigated the effects of Cr addition on the microstructures and the electrochemical performances of the $La_2Mg(Ni_{0.85}Co_{0.15})_9Cr_x$ ($x = 0–0.4$) alloys.

2. Experimental

The experimental alloys were melted in an argon atmosphere using a vacuum induction furnace. A positive argon pressure of 0.1 MPa was applied for preventing the volatilization of magnesium during melting. Part of the as-cast alloys was re-melted and quenched by melt-spinning with a rotating copper wheel. The quenching rate is expressed by the linear velocity of the copper wheel and the quenching rates used in the experiment are 15, 20, 25 and 30 m/s. The nominal composition of the investigated alloys is $La_2Mg(Ni_{0.85}Co_{0.15})_9Cr_x$ ($x = 0$, 0.1, 0.2, 0.3, 0.4), and corresponding with Cr content, the alloys are represented by Cr_0, Cr_1, Cr_2, Cr_3 and Cr_4, respectively.

A round electrode pellet 15 mm in diameter was prepared by mixing 1 g alloy powder with fine nickel powder in a weight ratio of 1:1 together with a small amount of polyvinyl alcohol (PVA) solution as binder, and then compressed under a pressure of 35 MPa.

The experimental electrodes were tested in a tri-electrode open cell, consisting of a metal hydride working electrode, a $NiOOH/Ni(OH)_2$ counter electrode and a Hg/HgO reference electrode. The electrolyte was a 6 M KOH solution. The cycle life of the alloy electrodes was measured by an automatic galvanostatic charging–discharging unit (30 °C). In each cycle, the negative electrode was charged with a current density of 100 mA/g for 5 h, resting 15 min and then discharged at 100 mA/g to a −0.500 V cut-off voltage.

The phase structures and composition of the alloys were determined by XRD diffractometer of D/max/2400. The diffraction was performed with Cu $K_{\alpha 1}$ radiation filtered by graphite. The experimental parameters for determining phase structure are 160 mA, 40 kV and 10°/min, respectively. The morphologies and the crystalline states of the as-quenched alloys were determined by TEM.

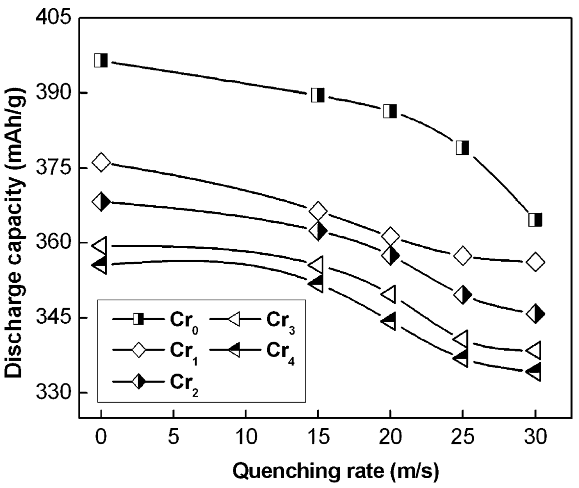

Fig. 1. Evolution of the discharge capacity of the alloys with the quenching rate.

3. Results and discussion

3.1. Effect of Cr addition on electrochemical performance

3.1.1. Discharge capacity

Fig. 1 illustrates the maximum discharge capacity of the alloys as a function of the quenching rate, and charge–discharge current density being 100 mA/g. It turns out that an increase of the quenching rate involves a notable decrease in the discharge capacity, and for a fixed quenching rate, the discharge capacity of the alloys decreases with incremental change of Cr content. When Cr content increased from 0 to 0.4, the discharge capacity of as-cast alloy reduced from 396.4 to 355.6 mAh/g, for the as-quenched (30 m/s) alloy from 364.6 to 334.2 mAh/g.

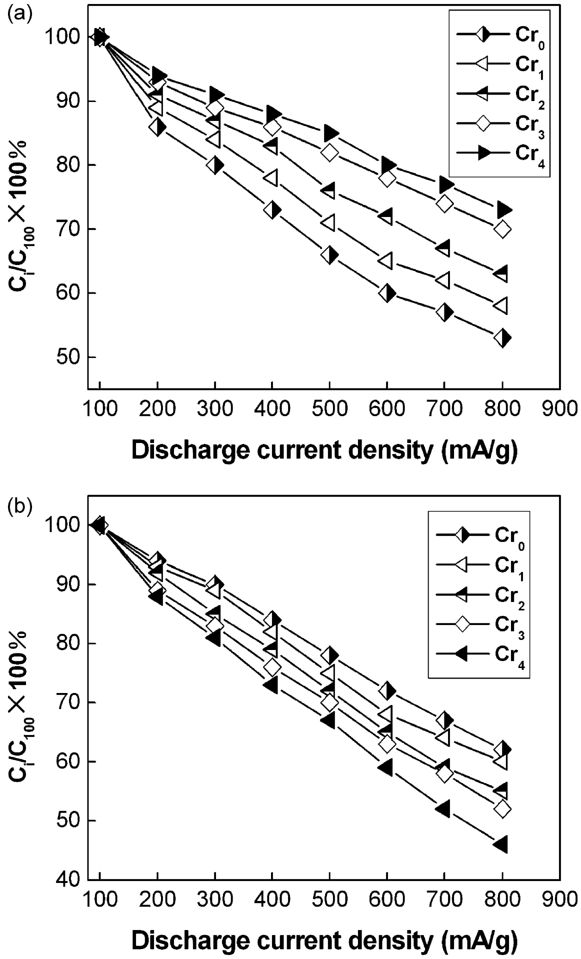

Fig. 2. The high rate discharge ability (HRD) of the as-cast and quenched (30 m/s) alloys: (a) as-cast; (b) as-quenched.

3.1.2. High rate discharge capability

The high rate discharge ability (HRD), which was determined mainly the kinetic property of the hydrogen storage alloy electrode, is defined and calculated according to the following formula: HRD = $C_i/C_{100} \times 100\%$, where C_i is the discharge capacity of the electrode discharged at the current density I_i, and C_{100} is the discharge capacity measured at a discharge current density of 100 mA/g. The discharge current density dependence of the HRD of the as-cast and quenched alloys is plotted in Fig. 2. It was seen in Fig. 2 that an increase of the discharge current density involves a significant reduction of the HRD of the as-cast and quenched alloys. For a fixed discharge current density, the HRD of the as-cast alloys clearly increases with increasing Cr content, and for the as-quenched alloys, the result is contrary. When Cr content increased from 0 to 0.4, the HRD of the as-cast alloys at 800 mA/g elevated from 53 to 73%, and for the as-quenched (30 m/s) alloys, it lowered from 62 to 46%.

3.1.3. Discharge potential characteristic

The discharge potential discussed in this section means its absolute value. The discharge potential curves of the as-cast and quenched alloys were shown in Fig. 3. The figure shows that the addition of Cr has an inconspicuous influence on the discharge potential characteristics of the as-cast alloys, but it lead to a significant decrease of the discharge potential of the as-quenched alloys. Comparing Fig. 3(a) to (b), it was derived

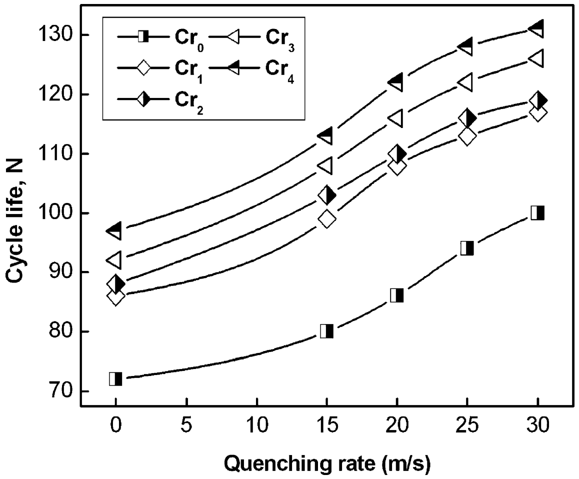

Fig. 4. Evolution of the cycle life of the alloys with the quenching rate.

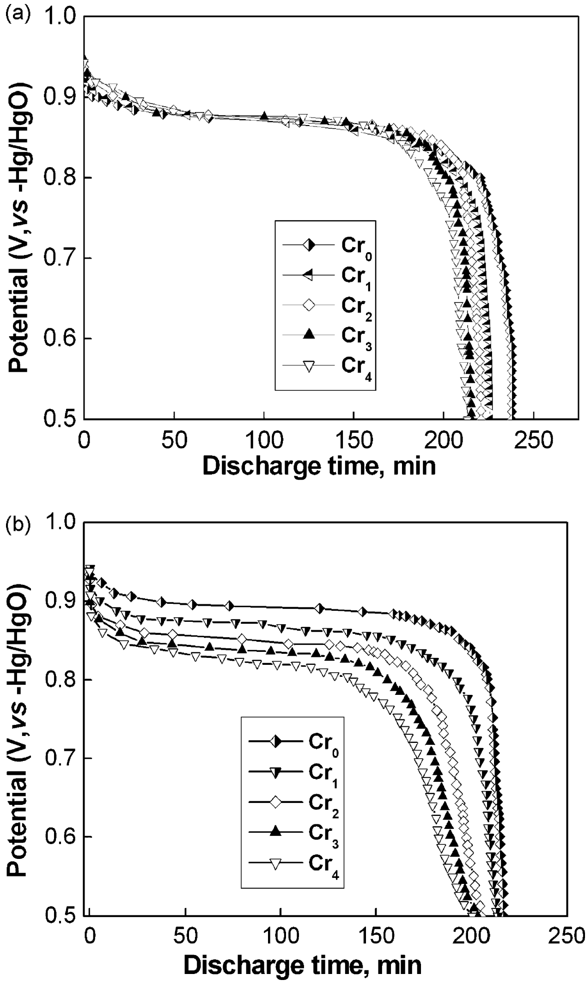

Fig. 3. The discharge potential curves of the as-cast and quenched (30 m/s) alloys: (a) as-cast; (b) as-quenched.

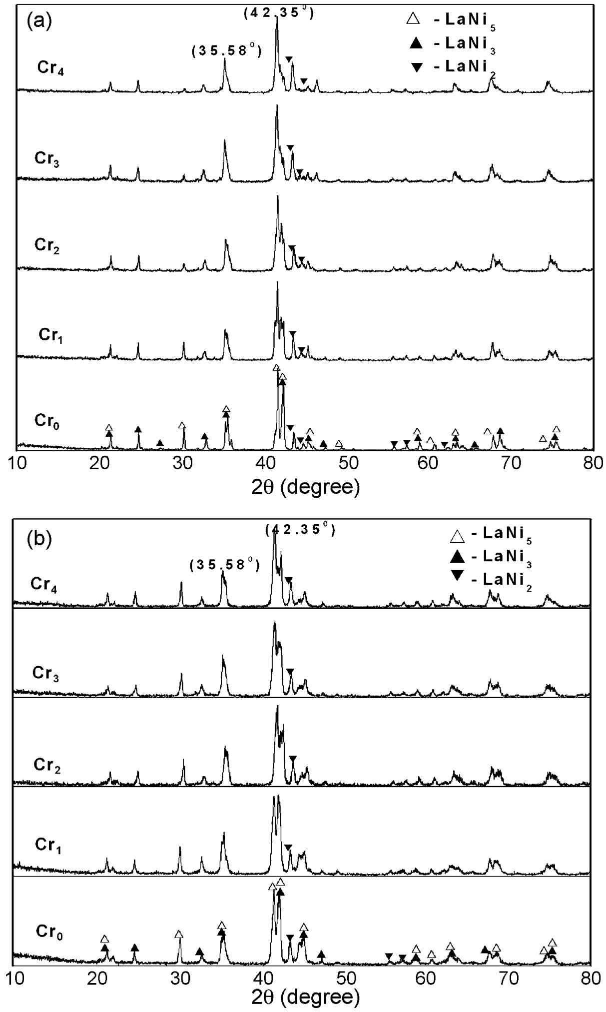

Fig. 5. The XRD patterns of the as-cast and quenched (30 m/s) alloys: (a) as-cast; (b) as-quenched.

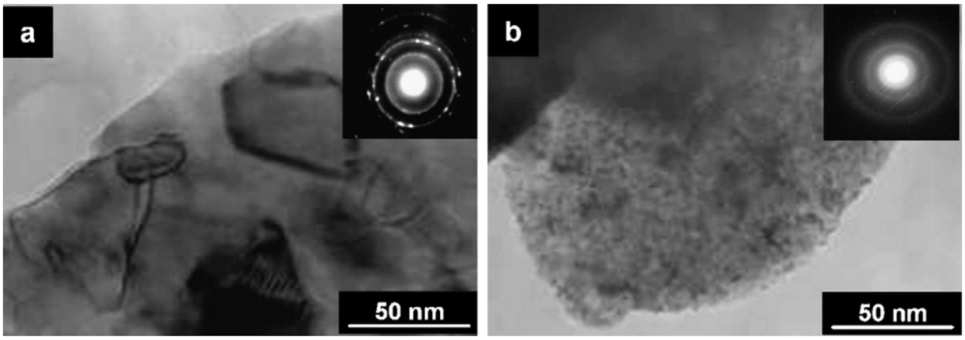

Fig. 6. The morphologies and SAD of the as-quenched (20 m/s) Cr_0 and Cr_3 alloys taken by TEM: (a) Cr_0 alloy; (b) Cr_3 alloy.

that rapid quenching clearly raises the discharge potential of the Cr-free alloy, but it markedly decreases the discharge potential and worsens the discharge potential characteristic of the alloys with Cr.

3.1.4. Cycle life

The cycle life, indicated by N, is characterized by the cycle number after which the discharge capacity of the alloy is reduced to 60% of the maximum capacity. The cycle life of the alloys as a function of the quenching rate was shown in Fig. 4. The cycle lives of the alloys were markedly prolonged with elevating quenching rate. When quenching rate was enhanced from 0 (as-cast was defined as quenching rate of 0 m/s) to 30 m/s, the cycle life of Cr_0 alloy extends from 72 to 100 cycles, and for Cr_4 alloy from 97 to 131 cycles. For a fixed quenching rate, the cycle life of the alloys significantly increases with the incremental change of Cr content. When Cr content varies from 0 to 0.4, the cycle life of the as-cast alloys enhanced from 72 to 97 cycles, and for the as-quenched (30 m/s) alloys, from 100 to 131 cycles.

3.2. Effect of Cr addition on microstructure

The XRD patterns of the as-cast and quenched alloys are shown in Fig. 5. All the alloys have a multiphase structure, composing of the (La, Mg)Ni_3, the $LaNi_5$ and the $LaNi_2$ phases. The FWHM values of the main diffraction peaks of the as-cast and quenched alloys, which were calculated by software of Jade 6.0 were listed in Table 1. It can be derived from Table 1 that rapid quenching produces broad diffuse peaks, indicating refinement of the average grain size and stored stress in the grains. The Cr addition does not have much influence on the phase composition of the as-cast and quenched alloys, but it leads to an obvious increase of the $LaNi_2$ phase in the as-cast alloys.

The morphologies and the crystalline state of the as-quenched alloys examined by TEM were shown in Fig. 6. As shown in Fig. 6, the selected area diffraction (SAD) of Cr_0 alloy displays a clear crystal characteristic, but it shows a strong tendency to form amorphous phase in the Cr_3 alloy, implying that the Cr addition is favourable for the formation of an amorphous phase.

The mechanism of the Cr addition reducing the discharge capacity of the as-cast and quenched alloys is different. For the as-cast alloy, it is mainly ascribed to the growth of the $LaNi_2$ phase. For the as-quenched alloy, it is mainly contributed to the formation of amorphous phase because the discharge capacity of amorphous phase is about half as large as that of the crystalline alloy [11].

The HRD of the alloys is a dynamical problem of the alloy electrode's absorbing/desorbing hydrogen. The grain refinement of the alloy produced by rapid quenching enhances the diffusion capability of hydrogen atoms in the alloy and raises the HRD of the alloy. The addition of Cr produces a completely different influence on the HRD of the as-cast and quenched alloys, for which Cr addition promoting the formation of an amorphous phase is responsible.

Cr addition improving the anticorrosion capability of the alloy is responsible for Cr addition enhancing the cycle stability of the as-cast alloy. The main reason of Cr addition improving the cycle stability of the as-quenched alloy is that the Cr addition accelerates the formation of an amorphous phase because an amorphous phase can enhance not only the antipulverization capability but also the anticorrosion performance of the alloy [12].

Table 1
The FWHM values of the diffraction peaks of as-cast and quenched (30 m/s) alloys

Alloys	FWHM values			
	2θ (42.35°)		2θ (35.58°)	
	As-cast	As-quenched	As-cast	As-quenched
Cr_0	0.167	0.374	0.182	0.256
Cr_1	0.181	0.405	0.221	0.359
Cr_2	0.214	0.432	0.231	0.473
Cr_3	0.365	0.442	0.239	0.535
Cr_4	0.330	0.620	0.319	0.609

4. Conclusions

1. The Cr addition engenders an inappreciable influence on the phase composition of the as-cast and quenched $La_2Mg(Ni_{0.85}Co_{0.15})_9Cr_x$ ($x = 0, 0.1, 0.2, 0.3, 0.4$) electrode alloys, but it increases the amount of the $LaNi_2$ phase in the as-cast alloys and is favourable for the formation of an amorphous phase in the as-quenched alloys.
2. The Cr addition significantly increases the cycle stability of the as-cast and quenched alloys, but it leads to a different extent decrease of the discharge capacity of the alloys. The Cr addition has a negligible influence on the dis-

charge potential characteristic of the as-cast alloys, whereas it clearly impairs the discharge potential characteristic of the as-quenched alloys. The HRD of the as-cast alloys increases with increasing Cr content, and for the as-quenched alloys, it is completely contrary.

Acknowledgements

This work is supported by National Natural Science Foundation of China (50642033), Science and Technology Planned Project of Inner Mongolia, China (20050205) and Higher Education Science Research Project of Inner Mongolia, China (NJ05064).

References

[1] Q.D. Wang, C.P. Chen, Y.Q. Lei, J. Alloys Compd. 253–254 (1997) 629–634.

[2] I. Uehara, T. Sakai, H. Ishikawa, J. Alloys Compd. 253–254 (1997) 635–641.

[3] T. Knhno, H. Yoshida, F. Kawashina, T. Inaba, I. Sakai, M. Yamamoto, M. Kanda, J. Alloys Compd. 311 (2000) L5–L7.

[4] B. Liao, Y.Q. Lei, L.X. Chen, G.L. Lu, H.G. Pan, Q.D. Wang, Electrochim. Acta 50 (2004) 1057–1063.

[5] K. Kadir, I. Uehara, T. Sakai, J. Alloys Compd. 257 (1997) 115–121.

[6] H.G. Pan, Y.F. Liu, M.X. Gao, R. Li, Y.Q. Lei, Intermetallics 13 (2005) 770–777.

[7] Akito Takasaki, Kazuya Sasao, J. Alloys Compd. 404–406 (2005) 431–434.

[8] H.G. Pan, Y.F. Liu, M.X. Gao, R. Li, Y.Q. Lei, Intermetallics 13 (2005) 770.

[9] Yang-Huan Zhang, Mei-yan Chen, Xiao-ping Dong, Guo-qing Wang, Xin-lin Wang, J. Alloys Compd. 376 (2004) 275–281.

[10] Yang-huan Zhang, Guo-qing Wang, Xiao-ping Dong, Shi-hai Guo, Xin-lin Wang, Int. J. Hydrogen Energy 30 (2005) 1091–1098.

[11] Y. Li, Y.T. Cheng, J. Alloys Compd. 223 (1995) 6–12.

[12] Yang-Huan Zhang, Guo-Qing Wang, Xiao-Ping Dong, Shi-Hai Guo, Jian-Min Wu, Xin-Lin Wang, J. Alloys Compd. 398 (2005) 178–183.